Influence of Discrete Heat Source Location on Natural Convection Heat Transfer in a Vertical Square Enclosure

G. Refai Ahmed
Research Assistant.
Student Member, ASME

M. M. Yovanovich
Professor of Mechanical Engineering and Electrical Engineering.
Fellow ASME

Microelectronics Heat Transfer Laboratory,
Department of Mechanical Engineering,
University of Waterloo,
Waterloo, Ontario, Canada N2L 3G1

A numerical study is carried out to investigate the influence of discrete heat sources on natural convection heat transfer in a square enclosure filled with air. The enclosure has two vertical boundaries of height H; one of them is cooled at T_c and the other has discrete heat sources [isoflux (q = c) or isothermal (T_h = c)]. The enclosure has two horizontal adiabatic boundaries of length L. Results are reported for $0 \leq Ra \leq 10^6$, $Pr = 0.72$, $A = 1$, aspect ratio ϵ, the relative size of the heat source to the total height, lies in the range $0.25 \leq \epsilon \leq 1$ and the discrete heat sources are located at the top or the bottom of the enclosure. Verification of numerical results is obtained at $Ra = 0$ (conduction limit) with analytical conduction solutions. In addition, a comparison with experimental and numerical data is made which also shows good agreement. The relationships between both Nu, ΔNu (change of thermal conductance) and Ra based on scale length (the size of the heat source S divided by the aspect ratio A) are also investigated here. A relationship Nu and Ra, based on scale length obtained from analytical solutions is correlated as $Nu = Nu(Ra, \epsilon)$. In addition, extrapolation correlations of Nu over the very high range of Rayleigh numbers ($Ra \geq 10^8$) are developed.

1 Introduction

The influence of discrete heat source size and location and boundary conditions on natural convection heat transfer within a square enclosure filled with air, is investigated in this work using a numerical finite difference technique.

The enclosure, as shown in Fig. 1, consists of two vertical boundaries of height H, and two horizontal boundaries of length L. One vertical boundary is maintained at T_c and the other has a discrete heat source (isoflux q or isothermal T_h) on an otherwise adiabatic surface. The top and bottom horizontal boundaries are adiabatic.

There are few investigations which have examined the effect of location of the discrete heat source inside the square cavity. Chu and Churchill [1] were the first to study this problem numerically. They examined the effect of the location in the range of Ra_H from 0 to 10^5. Chu and Churchill [1] found that Nu_s was proportional to Ra_H for any location of the discrete heat source. Flack and Turner [2] and Turner and Flack [3] also studied the previous effect experimentally but at high Rayleigh number (based on the cavity height) for $4.3 \times 10^6 \leq Ra_H \leq 6.48 \times 10^6$ and confirmed the observations of Chu and Chruchill [1]. Recently, Cesini et al. [4] studied the effect of the location of the discrete heat source numerically and experimentally with the discrete heat source at the bottom or center of the wall and reported the same observations as the previous studies [1-3]. However, the difference between Cesini et al. [4] and Chu and Churchill [1] at $A = 1$, $\epsilon = 0.5$, $P/H = 0.5$ and $Ra_H = 2.5 \times 10^4$, was approximately -5 percent and between Cesini et al. [4] and Turner and Flack [3] at $A = 1$, $\epsilon = 0.5$, $P/H = 0.5$ and $Ra_H = 3 \times 10^5$, was approximately, 18 percent. These comparisons are based on the results of Cesini et al. [4].

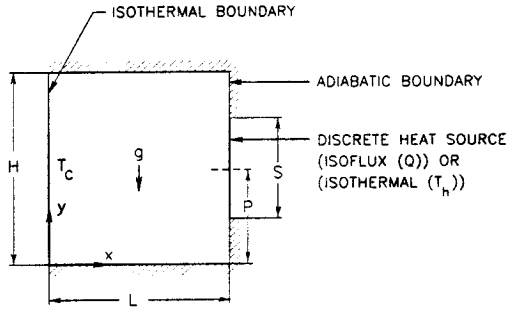

Fig. 1

The objectives of this study are to examine the effect of the location of the discrete heat source on the rate of heat transfer in the range of Ra (based on S/A) from 0 to 10^6, and also to examine the effect of boundary conditions of the discrete heat

Contributed by the Electrical and Electronics Packaging Division for publication in the JOURNAL OF ELECTRONIC PACKAGING. Manuscript received by the EEPD March 1, 1990, revised manuscript received March 15, 1991. Associate Editor: W. Z. Black.

source (IFDHS or ITDHS). Finally, examination of the scale length (S/A) is made, which was developed analytically by Refai and Yovanovich [5] in order develop design correlations for this problem. Design correlations in microelectronics applications are required to cover the high range of the Rayleigh number.

This paper is organized as follows. In the following section, the governing equations are stated with proper assumptions. In the third section, the definition of the Nusselt number is given. In section 4, the numerical technique is presented and the numerical results are discussed. In addition, the obtained and correlated results are discussed in section 4. Finally, conclusion are given in section 5.

2 The Governing Equations

The flow is assumed to be laminar, two-dimensional, and incompressible with constant density except in the buoyancy term of the momentum equation (the Boussinesq approximation). The nondimensionalized governing equations are:

$$\frac{\partial U}{\partial X}+\frac{\partial V}{\partial Y}=0 \tag{1}$$

$$\frac{DU}{D\tau}=-\frac{\partial P_d}{\partial X}+Pr\,\nabla^2 U \tag{2}$$

$$\frac{DV}{D\tau}=-\frac{\partial P_d}{\partial Y}+Pr\,\nabla^2 V+\mathrm{RaPr}\Theta \tag{3}$$

$$\frac{D\Theta}{D\tau}=\nabla^2\Theta \tag{4}$$

with the nondimensional variables defined as:

$$U=\frac{u(S/A)}{\alpha}\quad V=\frac{v(S/A)}{\alpha}\quad \tau=\frac{t\alpha}{(S/A)^2}$$

$$X=\frac{x}{(S/A)}\quad Y=\frac{y}{(S/A)}\quad P_d=\frac{p_d(S/A)^2}{\rho\alpha^2A^2}$$

$$\Theta=\frac{T-T_c}{T_h-T_c}\quad \text{ITDHS}$$

$$\Theta=\frac{(T-T_c)k}{q(S/A)}\quad \text{IFDHS}$$

The scale length S/A was obtained by Refai and Yovanovich [5] from the analytical solution at Ra = 0. This scale length is defined by common parameters that do not change within the rectangular enclosure (i.e., at $A \geq 1$ and $\epsilon = 1$ the scale length is L). In addition, this scale length S/A is consistent with the physics of the problem, where Nu increases with increasing ϵ. Finally, it brings together natural convection results of various sizes of heat sources; therefore, it should be easier to develop design correlations.

The nondimensional initial and boundary conditions are given as:

$$\begin{array}{lllll}
\tau=0: & & U=V=0 & & \Theta=0 \\
\tau\geq 0: & X=0 & U=V=0 & 0\leq Y\leq Y_3 & \Theta=0 \\
& X=\dfrac{LA}{S} & U=V=0 & 0\leq Y\leq Y_1 & \dfrac{\partial\Theta}{\partial X}=0 \\
& & & Y_1\leq Y\leq Y_2 & \dfrac{\partial\Theta}{\partial X}=1 \quad \text{IFDHS} \\
& & & Y_1\leq Y\leq Y_2 & \Theta=1 \quad \text{ITDHS} \\
& & & Y_2\leq Y\leq Y_3 & \dfrac{\partial\Theta}{\partial X}=0
\end{array}$$

$$0\leq X\leq\frac{LA}{S}\quad U=V=0\quad Y=0 \text{ and } Y_3\frac{\partial\Theta}{\partial Y=0}$$

3 Definition of the Nusselt Number

The local and average thermal energy balances at $x = L$ give the local heat transfer coefficient:

$$h_y\theta s=k\frac{\partial\theta}{\partial x} \tag{5}$$

and the average value:

$$h=\frac{k}{S\bar{\theta}_s}\int_{P-\frac{S}{2}}^{P+\frac{S}{2}}\frac{\partial\theta}{\partial x}dy \tag{6}$$

Nomenclature

A = aspect ratio of cavity, $A=H/L$
As = surface area per unit length, m
C_p = specific heat at constant pressure, kJ/kg•K
g = gravitational acceleration, m/s^2
H = height of the cavity, m
h = total coefficient of heat transfer, W/m^2•K
h_{cond} = coefficient of heat transfer by conduction, Eq. (19), W/m^2•K
h_{conv} = coefficient of heat transfer by convection, Eq. (19), W/m^2•K
h_y = local coefficient of heat transfer, W/m^2•K
k = thermal conductivity, W/m•K
L = width of cavity, m
Nu = average Nusselt number, $\mathrm{Nu}=h(S/A)/k$
Nu_s = average Nusselt number, $\mathrm{Nu}=hS/k$
P = distance from the bottom of the enclosure, m
P_d = non-dimensional dynamic pressure
p_d = dimensional dynamic pressure, N/m^2
Pr = Prandtl number, $\mathrm{Pr}=\nu/\alpha$
Q = total heat flow rate per unit length, W/m
Q_{cond} = conduction heat flow rate per unit length, W/m
Q_{conv} = convection heat flow rate per unit length, W/m
Q_{loss} = lead losses per unit length, W/m
Q_{rad} = radiation heat flow rate per unit length, W/m
q = heat flux, W/m^2
Ra = Rayleigh number, $\mathrm{Ra}=(S/A)^3\beta g(T_h-T_c)/\alpha\nu$
Ra_H = Rayleigh number, $\mathrm{Ra}=H^3\beta g(T_h-T_c)/\alpha\nu$
Ra* = isoflux Rayleigh number, $\mathrm{Ra}^*=(S/A)^4\beta gq/\alpha\nu k$
R_c = nondimensional constriction resistance, $R_c=R_t-R_m$,
R_m = nondimensional material resistance, $R_m=r_m\bullet k\bullet A\bullet$ (unit length)
r_m = material resistance, $r_m=1/[k\bullet A\bullet$(unit length)], K/W
R_t = nondimensional total resistance, $R_t=\bar{\theta}_s k/q(S/A)$
S = length of discrete heat source, m
T = temperature, K
T_m = mean temperature, $T_m=(\bar{T}_h+T_c)/2$, K
t = time, s
U = nondimensional velocity component in X direction
u = dimensional velocity component in x direction, m/s

Table 1 Comparison between numerical and analytical solutions (IFDHS) at Ra = 0†

ϵ		R_c	R_m	R_t	ΔR_t%
	*	0.67	.999	1.67	
0.25					0.6
	•	0.68	1.0	1.68	
	*	0.259	.999	1.258	
0.50					0.8
	•	0.27	1.0	1.27	
	*	0.067	0.999	1.066	
0.75					0.1
	•	0.067	1.0	1.067	
	*	0.0	0.999	0.999	
1.0					0.02
	•	0.0	1.0	1.0	

† More detail about R_c, R_m and R_t in [5]
* Numerical Results
• Analytical Results

Table 2 Comparison between numerical and analytical solutions (ITDHS) at Ra = 0

ϵ		R_c	R_m	R_t	ΔR_t%
	*	0.636	0.999	1.635	
0.25					−0.8
	•	0.622	1.0	1.622	
	*	0.236	0.999	1.2348	
0.50					−0.8
	•	0.225	1.0	1.225	
	*	0.05752	0.999	1.057	
0.75					−0.4
	•	0.052	1.0	1.052	
	*	0.0	0.999	0.999	
1.0					0.02
	•	0.0	1.0	1.0	

* Numerical Results
• Analytical Results

The total heat flow rate at $x = L$, is therefore,

$$Q = q \cdot S = k \int_{P-\frac{S}{2}}^{P+\frac{S}{2}} \frac{\partial \theta}{\partial x} dy = h \cdot S \cdot \bar{\theta}_s \tag{7}$$

The area-average Nusselt number can be defined as:

$$\mathrm{Nu} = \frac{h(S/A)}{k} = \frac{q(S/A)}{k\bar{\theta}_s} \tag{8}$$

which is based on the scale length S/A.

4 Results and Discussion

A numerical finite difference technique,the Marker and Cell method MAC, developed by Harlow and Welch [6], is modified to solve the governing Eqs. (1-4). This method uses a finite difference formulation with primitive variables as the de pendent variables. More details how to apply this technique to this problem are given in [5, 7]. In the present study, the air layer was divided into (24 × 24) cells which are surrounded by a single layer of boundary cells marking the computational matrix (26 × 26). The steady-state solution was obtained as the limit of the transient calculations using a nondimensional time step, $\Delta\tau$ as low as 8×10^{-5}. This gave an average computational time per cell per time step of about 0.002s on a PC AT 386 ($A = 1$, $\mathrm{Ra} = 10^6$, $\epsilon = 1$, IFDHS). Also by increasing the number of cells up to 38 × 38, a slight difference (approximately 0.9 percent) between the average Nusselt number was found.

Before studying the effect of the different parameters on the average Nusselt number, it was necessary to examine the accuracy or the MAC technique; this test was reported in more detail by Refai and Yovanovich [5]. This study contains only the comparison between the numerical solution and the analytical results when the discrete heat source is located at the top or the bottom of the enclosure as shown in Tables 1 and 2. The total resistance R_t consists of the material resistance R_m and the constriction resistance R_c. The material resistance depends upon the geometry of the enclosure, while the constriction resistance is a function of the size and the location of the discrete heat source as shown in Tables 1 and 2.

Remark 1

There is very good agreement within 1 percent, between the

Nomenclature (cont.)

V = nondimensional velocity component in Y direction
v = dimensional velocity component in y direction, m/s
X = nondimensional coordinate
x = dimensional coordinate, m
Y = nondimensional coordinate
Y_1 = nondimensional length, [(PA/A) − 0.5A]
Y_2 = nondimensional length, [(PA/S) + 0.5A]
Y_3 = nondimensional length, [HA/S]
y = dimensional coordinate, m
α = thermal diffusivity, $\alpha = k/C_p\rho$, m^2/s
β = coefficient of thermal expansion, 1/K
$\Delta\mathrm{Nu}$ percent = $[(\mathrm{Nu}_{\mathrm{Eq.\ (13)}} - \mathrm{Nu}_{\mathrm{ref}})/\mathrm{Nu}_{\mathrm{Eq.\ (13)}}] \times 100$ percent
ΔR_t percent = $[(R_{t_{\mathrm{anal}}} - R_{t_{\mathrm{num}}})/R_{t_{\mathrm{anal}}}] \times 100$ percent
ϵ = relative discrete heat source size, $\epsilon = \mathrm{S/H}$
ρ = density, kg/m^3
ν = kinematic viscosity, m^2/s
τ = nondimensional time
Θ = nondimensional temperature
$\Theta = T - T_c/T_h - T_c$ or
$\Theta = (T - T_c)_k/q(S/A)$
θ = temperature excess, $\theta = T - T_c$, K
$\bar{\theta}_s$ = area-average source temperature excess, $\bar{\theta}_s = \bar{T}_s - T_c$, K

Subscripts

anal = analytical solution
c = cold temperature
cond = conduction
conv = convection
exp = experimental
H = height of the cavity
h = hot temperature
num = numerical solution
rad = radiation
ref = reference number
S = discrete heat source

Abbreviations

IFDHS = isoflux discrete heat source
ITDHS = isothermal discrete heat source
MAC = Marker and Cell

Mathematical Expressions

$$\frac{D}{D\tau} = \frac{\partial}{\partial\tau} + U\frac{\partial}{\partial X} + V\frac{\partial}{\partial Y}$$

$$\nabla^2 = \frac{\partial^2}{\partial X^2} + \frac{\partial^2}{\partial Y^2}$$

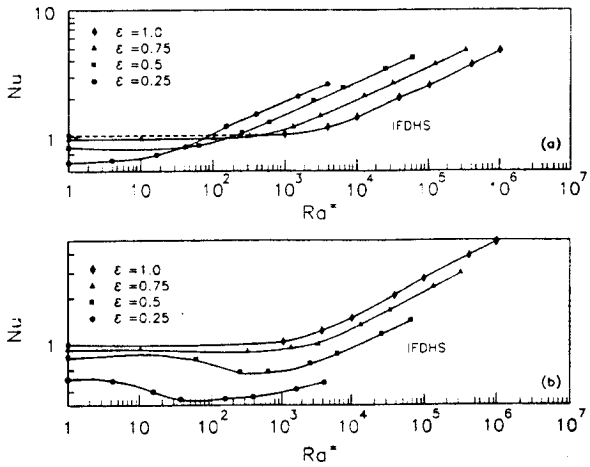

Fig. 2

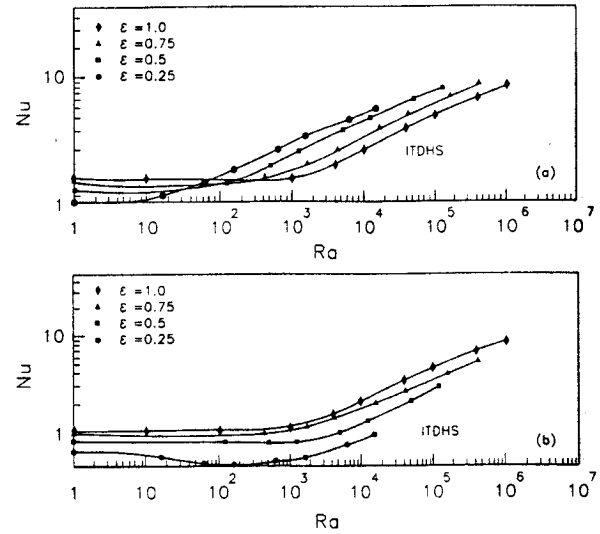

Fig. 3

numerical results and the analytical solutions for R_t at Ra = 0.

Figures 2 and 3 show the relationships between the Nusselt number and the Rayleigh number for IFDHS and ITDHS, respectively. The location of the discrete heat source is varied between the bottom and top of the right vertical boundary. The trend of the relationships between Nu and Ra* or Ra as shown in Figs. 2(*a*) and 3(*a*), when the discrete heat source is at the bottom of the wall, is the same as the trend when the discrete heat source is at the center of the wall, which was studied by Refai and Yovanovich [5]. It is found that when Ra* or Ra is greater than 300, Nu decreases with increasing ϵ. In contrast, when the discrete heat source is at the top as shown in Figs. 2(*b*) and 3(*b*), Nu decreases with increasing Rayleigh number up to a certain value (approximately at Rayleigh equal 300). Chu and Churchill [1] found that Nu_s increases at any location of the discrete heat source with Ra_H. However a cautionary remark, Yaghoubi and Incropera [8] state that the coarse mesh of Chu and Churchill [1] can lead to spurious flows, even with computational stability.

In addition, ElSherbiny [9] determined experimentally the effect of location (full contact heat source $\epsilon = 1$) using three heaters on the hot wall. He measured Nu for each heater; Nu for the upper heater was found to decrease up to a certain Ra and then increase again, as shown in Fig. 4. Figure 4 also

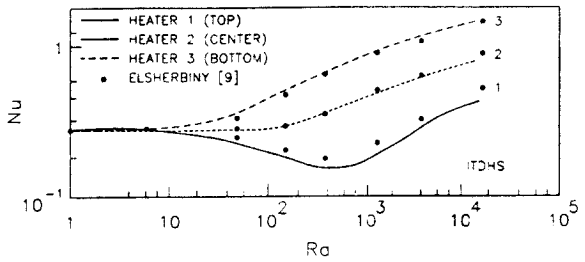

Fig. 4

Table 3 Comparison Between Results of Cesini et al. [4] and Present Study at $P/H = 0.25$ and $\epsilon = 0.5$

Ra	Cesini et al.	Present study	Diff.%[†]
5×10^3	2.75	3.00	8.2
1.25×10^4	3.62	3.97	8.8
5×10^4	5.49	5.92	7.3

[†] Diff.% = $[(Nu_{[present]} - Nu_{[4]})/Nu_{[present]}] \times 100\%$

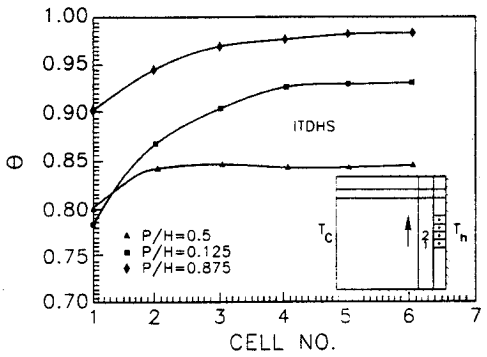

Fig. 5

shows the comparison between the present results and El-Sherbiny [9]. The trend of the relationships between the Nusselt number and the Rayleigh number is the same, and there is good agreement between [9] and this study.

Table 3 shows the comparision between the present results and the correlation of the numerical results of Cesini et al. [4] for $\epsilon = 0.5$ and $P/H = 0.25$. The average difference is -8 percent. However the maximum difference between the correlation of Cesini et al. [4] and their experimental work was 17 percent (their numerical results are higher than their experimental data). They suggest that this difference is probably due to the difficulties in interpreting the interferograms near the bottom corner of the enclosure, due to the high concentration of fringes. Furthermore the effect of thermal conduction of the insulating walls should be taken into consideration.

Refai and Yovanovich [5] also showed very good agreement between their numerical results and the experimental results of MacGregor and Emery [10], and Eckert and Carlson [10] when $\epsilon = 1$.

Figure 5 shows the variation of the air temperature profiles at the first column of cells away from the smallest discrete heat source ($X = 0.98$, $\epsilon = 0.25$) for Ra = 625. The trend of the temperature profiles is identical at any location of the discrete heat source. It usually starts at a low temperature and increases. However, the average temperatures are 0.836, 0.891 and 0.96 (*bottom, center, top*). The increase in the average temperature with increase in elevation implies there is a decrease in the heat transfer coefficient or average Nusselt number. Figure 6 also shows the variation of the temperature profiles

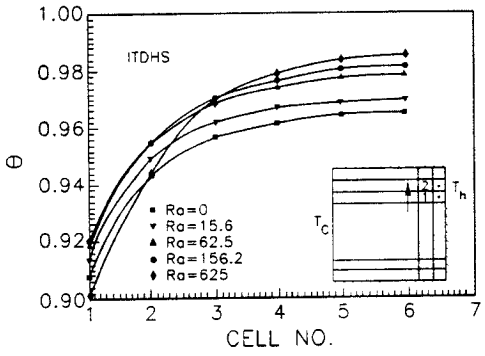

Fig. 6

at the first column of cells away from the smallest discrete heat source ($\epsilon = 0.25$) when it is located at the top for various Rayleigh number ($0 \le Ra \le 625$) and ITDHS. The trend of the temperature profiles is the same as in Fig. 5. However, the temperature increases with increasing Rayleigh number ($0 \le Ra \le 62.5$). After this the distribution of the temperature at the bottom of the discrete heat source decreases with increasing Ra. Therefore Nu decreases to $Ra = 62.5$ and then decreases when the cooling layer begins moving to the top of the enclosure.

The relationship between ΔNu and the Rayleigh number was developed by Refai and Yovanovich [5] (see Appendix), to assist in the development of correlations of $Nu = Nu(Ra, \epsilon)$ or $Nu = Nu(Ra^*, \epsilon)$ and to make it possible to extrapolate to very large Ra. The change in Nusselt, ΔNu, due to fluid motion is defined by the following equation:

$$\Delta Nu + Nu(Ra = 0) = Nu(Ra) \tag{9}$$

Figures 7 and 8 show this relationship for both IFDHS and ITDHS when the discrete heat source is located at the top and then the bottom of the enclosure. ΔNu increases with increasing Rayleigh and all curves of ΔNu approach a common asymptote (approximately at $Ra = 10^8$). This asymptote is the curve of the full contact heat source $\epsilon = 1$. (Refai and Yovanovich [5] also obtained this asymptote when the discrete heat source was located at the center of the enclosure). Therefore there is negligible effect of the size of the discrete heat source for $Ra > 10^8$.

Remark 2

The relationships between ΔNu and Ra and Ra approach a common asymptote. This asymptote is the same whether the discrete heat source is located at the top, center [5] or bottom. Therefore, there is negligible effect of the location or the size of the discrete heat source at high Rayleigh number ($Ra > 10^8$).*

It is very important to correlate numerical data, since it is difficult, if not impossible, to use the results otherwise. If the design equation is general, it will be more useful in engineering applications. In microelectronics applications, correlations are required to cover the high range of the Rayleigh number. Refai and Yovanovich [5] developed two equations to cover the range of $0 \le Ra \le 10^6$, when the discrete heat source (IFDHS) or (ITDHS) is at the center by using the blending method of Churchill and Usagi [12]. These equations are also applicable when the discrete heat source is located at the bottom by slight modifications as follows:

1 IFDHS, $0 \le Ra^* \le 10^6 \epsilon^4$

$$Nu = \left[\epsilon^{1.511}(\epsilon^{1.294})^m + (0.21\epsilon^{-0.288}(Ra^*)^{0.221}[1.262(0.7)^n\epsilon^{-.012}]^m)^{\frac{17}{2}} \right]^{\frac{2}{17}} \tag{10}$$

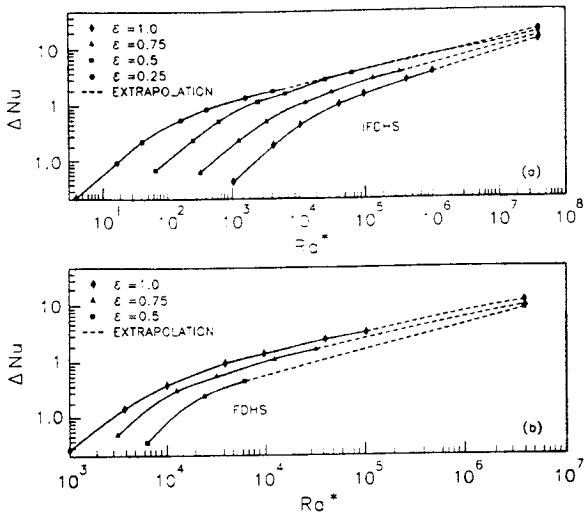

Fig. 7

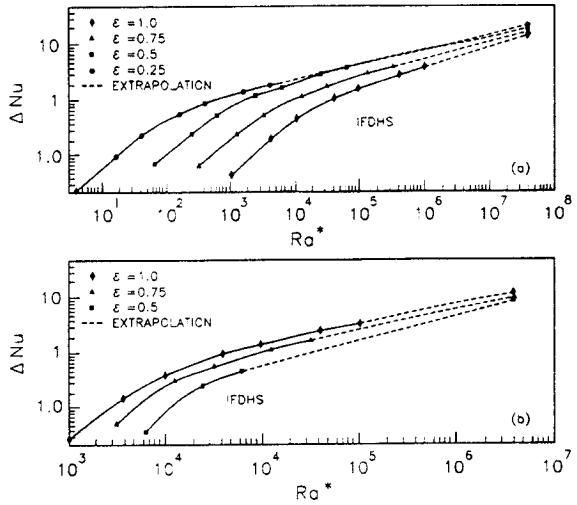

Fig. 8

2 ITDHS, $0 \le Ra \le 10^6 \epsilon^3$

$$Nu = \left[\epsilon^{1.7}(\epsilon^{1.105})^m + (0.146\epsilon^{-0.256}Ra^{0.287}[1.25\epsilon^{-.0131}]^m)^{\frac{17}{2}} \right]^{\frac{2}{17}} \tag{11}$$

where m has two values:

(i) $m = 0$ when the discrete heat source is at the center or $\epsilon = 1$

(ii) $m = 1$ when the discrete heat source is at the bottom and n also has two values only when the discrete heat source is at the bottom:

(i) $n = 0$ for $0.5 \le \epsilon \le 1$

(ii) $n = 1$ for $\epsilon = 0.25$.

The maximum difference of 10 percent between the correlation equations and the numerical results occurs when Nu lies near the intersection of the conduction and laminar regime asymptotes. The average difference is 4.7 percent and the standard deviation is 2.1 percent. However, when the discrete heat source is located at the top, it is difficult to correlate the relationships between Nu and Ra, because Nu first decreases and then increases with increasing Ra. Figures 7 and 8 show that the relationships between ΔNu and Rayleigh number go to one asymptote for $\epsilon = 1$ at high Rayleigh number ($Ra \ge 10^8$). Therefore the extrapolation equations for IFDHS and

Table 4 Comparison between present study and previous numerical and experimental studies at $A = 1$ and $\epsilon = 1$ (ITDHS)

Ra	Eq.(13)	Nobile$_{num}$		Markatos$_{num}$		Abrams$_{num}$		Catton$^{1}_{exp}$		Cowan$^{2}_{exp}$	
	Nu	Nu	ΔNu%†	Nu	ΔNu%	Nu	ΔNu%	Nu	ΔNu%	Nu	ΔNu%
10^7	16.7	16.9	−1.2	—	—	16.2	3	17.7	−5.9	15.6	6.6
5×10^7	28.6	25.5	10.8	—	—	—	—	28.3	1.0	26.7	6.6
10^8	36.2	30.2	16.5	32.05	11.5	35.6	1.6	34.6	4.4	33.6	7.2
5×10^8	62.8	45.2	28.0	—	—	—	—	55.1	12.3	57.5	8.4
10^9	79.8	54.7	31.5	—	—	67.3	15.7	67.4	15.5	72.5	9.1
5×10^9	139.4	87.2	37.4	—	—	—	—	107.5	22.9	124	11
10^{10}	176.0	104.1	40.8	156.85	10.8	160.4	8.9	131.4	25.3	156	11.3

1 $Nu = 0.18[(Ra \cdot Pr)/(0.2 + Pr)]^{0.29}$
2 $Nu = 0.0725Ra^{0.33}$ where $(Pr = 0.72)$
$^{\dagger}\Delta Nu\% = [(Nu_{Eq.\ (13)} - Nu_{ref})/Nu_{Eq.\ (13)}] \times 100\%$

ITDHS of Refai and Yovanovich [5] are valid here with some modifications in the conduction and laminar limits.

The correlations are listed below for discrete heat sources at top, center or bottom, for $Ra \geq 10^8$.

For $10^8 \leq Ra^*$, the isoflux correlation equation is

$$Nu = \epsilon^{0.2}[\epsilon^{0.14}]^m + 0.0227(Ra^*)^{0.37} \quad (12)$$

For $10^8 \leq Ra$, the isothermal correlation equation is

$$Nu = \epsilon^{0.2}[\epsilon^{0.13}]^m + 0.0558Ra^{0.35} \quad (13)$$

where m has two values:

(i) $m = 0$ when the discrete heat source is at the center

(ii) $m = 1$ when the discrete heat source is at the bottom or the top.

One should not use Eqs. (12) and (13) when $[10^6\ \epsilon^4 \leq (Ra^*$ or $Ra) \leq 10^8]$ at $\epsilon < 1$, where the difference is 34 percent for $\epsilon = 0.5$, $P/H = 0.25$ at $Ra = 10^6$. However, one can use Figs. 7 and 8 in this range and then add the effect of conduction from Tables 1 or 2 ($Nu(Ra = 0) = 1/R_t$). For example at $\epsilon = 0.5$, $Ra = 10^6$, ITDHS and $P/H = 0.25$, ΔNu from Fig. 8(*a*) is 11.2 and Nu is 12.

Table 4 shows the comparison between Eq. (13), the present study, and the previous numerical and experimental studies [13–17]. This comparison shows that there is reasonable agreement in the range of Rayleigh number $10^7 \leq Ra \leq 10^8$ between the previous studies [13–17] and the present investigation. On the other hand, in the Rayleigh number range of $10^8 < Ra \leq 10^{10}$ the difference between the present results and the previous studies lies between 8.4 percent and 40.8 percent. Table 4 showns the Eq. (13) gives good predictions of Nusselt number over the range of Rayleigh number $10^7 \leq Ra \leq 10^{10}$; however, the physical interpretation is unknown.

Remark 3

The correlation equations, Eqs. (12) and (13), are in very good agreement with the results of previous experimental studies of MacGregor and Emery [10] and Eckert and Carlson [11] as shown in the study of Refai and Yovanovich [5], where they developed extrapolation equations for discrete heat sources at the center, i.e., without $[\ ]^m$.

5 Conclusions

The relationship between Nu and Ra has the same trend whether the discrete heat source is located at the center or bottom, but, when the discrete heat source is at the top, Nu decreases up to Ra = 300 and then increases. There is agreement between this observation when the discrete heat source is at the top and the investigation of ElSherbiny [9].

In addition, there is agreement between the experimental and numerical work of Cesini et al. [4] and the present study. In addition, Table 4 also shows the agreeement between the present study and the previous numerical and experimental studies [13–17] at high Rayleigh number; however, the physical interpretation is unknown.

The relationships between ΔNu and Ra show that, when $Ra > 10^8$ there is negligible effect of the relative size of the discrete heat source. This was also observed [5] for discrete heat sources located at the center ($P/H = 0.5$). Therefore, at high Rayleigh numbers ($Ra > 10^8$), there is negligible effect of the relative size of the discrete heat source at any location of the enclosure ($A = 1$) on the rate of heat transfer. The problem is similar to the full contact heat source ($\epsilon = 1$).

This study has also led to design correlations which are valid for any location of the discrete heat source, and for the range of Rayleigh number $0 \leq Ra < 10^{10}$.

6 Acknowledgments

The authors wish to acknowledge the financial support of the Natural Sciences and Engineering Research Council of Canada under grant No. A7455.

References

1 Chu, H. H., And Churchill, "The Effect of Ratio and Boundary Conditions on Two-Dimensional Laminar Natural Convection in Rectangluar Channels," ASME *Journal Heat Transfer*, Vol. 98, No. 2, 1976 pp. 194–201.

2 Flack, R. D., and Turner, B. L., "Heat Transfer Correlations for Use in Naturally Cooled Enclosures with High-Power Integrated Circuits," *IEEE Trans., on Components, Hybrids and Manufacturing Technology*, Vol. CHMT-3, 1980, pp. 449–452.

3 Turner, B. L., and Flack, R. D., "The Experimental Measurement of Natural Convection Heat Transfer in Rectangular Enclosures with Concentrated Energy Sources," ASME *Journal Heat Transfer*, Vol. 102, No. 2, 1980, pp. 236–241.

4 Cesini, G., Paromcini, M., and Ricci, R., "Experimental and Numerical Investigation on Natural Convection in Square Enclosures with a Non-Uniformly Heated Vertical Surface," *ICHMT XXth International Symposium*, Dubrovnik, Yugoslavia, 1988.

5 Refai Ahmed, G., and Yovanovich, M. M., "Numerical Study of NaturalConvection From Discrete Heat Sources in a Vertical Square Enclosure," AIAA 28th Aerospace Science Meeting, Reno NV, paper No. 90-0256, accepted and to appear in *J. Thermophysics and Heat Transfer*, Oct. 1991.

6 Harlow, F. H., and Welch, J. E., "Numerical Calculation of Time-Dependent Viscous Imcompressible Flow of Fluid with Free Surface," *J. Phys. of Fluids*, Vol. 8, 1965, pp. 2182–2189.

7 Fath, H. E. S., ElSherbiny, S. M., and Refai, G., "Influence of Prandtl Number and Boundary Condition Heat Transfer in Vertical and Inclined Fluid Layers," 88-HTD-99, ASME Winter Annual Meeting, Chicago, 1988, pp. 17–22.

8 Yaghoubi, M. A., and Incropera, F. P., "Analysis of Natural Convection Due to Localized Heating in a Shallow Water," ASME *J. Heat Transfer*, Vol. 101, 1980, pp. 569–571.

9 ElSherbiny, S. M., 1980, " Heat Transfer by Natural Convection Across Vertical and Inclined Air Layers," Ph.D., Department of Mechanical Engineering, University of Waterloo, Waterloo, Ont., Canada, 1980.

10 MacGregor, R. K., and Emery, A. F., "Free Convection Through Vertical Plane Layers-Moderate and High Prandtl Number Fluids," ASME *J. Heat Transfer*, Vol. 91, 1969, pp. 391–403.

11 Eckert, E. R. G., and Carlson, W. D., "Natural Convection in an Air Layer Enclosed Between Two Vertical Plates with Different Temperatures," *Int. J. Heat Transfer*, Vol. 2, 1961, pp. 106–120.

12 Churchill, S. W., and Usagi, R., 1972, "A General Expression for the Correlation of Rates of Transfer and Other Phenomena," *J. AIChE*, Vol. 18, No. 6, 1972, pp. 1121–1128.

12 Nobile, E., Sousa, A. C. M., and Barozzi, G. S., "Turbulent Buoyant

Flows in Enclosures," *Heat Transfer 90*, Vol. 2, Ed. G. Hetsroni, Hemisphere Publ. Corp. 1990, pp. 543-548.
14 Abrams, A., and Emery, A. F., "Turbulent Free Convection in Square Cavities with Mixed Boundary Conditions." Heat Transfer in Convection Flows, HTD-107, 1989, pp. 117-127.
15 Catton, I., "Natural Convection in Enclosures," *Proc. 6th International Heat Transfer Conference*, Toronto, Vol. 6, 1978, pp. 13-43.
16 Markatos, N. C., and Pericleous, K. A., "Laminar and Turbulent Natural Convection in an Enclosed Cavity," *Int. J. Heat and Mass Transfer*, Vol. 27, 1984, pp. 755-772.
17 Cowan, G. H., Lovegrove, P. C., and Quarini, G. L., "Turbulent Natual Convection Heat Transfer in Vertical Single Water-Filled Cavities," *Proc. of the 7th Int. Heat Transfer Conference*, Munich, Vol. 22, 1982 pp. 195-203.

APPENDIX

The total heat transfer, Q, consists of: conduction, Q_{cond}; convection, Q_{conv}; radiation, Q_{rad}; and lead losses, Q_{loss} therefore,

$$Q = Q_{cond} + Q_{conv} + Q_{rad} + Q_{loss} \tag{14}$$

We consider that Q_{loss} is negligible for this discussion. Also, we will assume that the top and bottom boundaries of the enclosure are adiabatic and the two vertical plates in the left and the right sides are isothermal, $\epsilon = 1$. Furthermore, Q_{rad} will be neglected.
Therefore,

$$Q = Q_{cond} + Q_{conv} \tag{15}$$

From the Fourier equation

$$Q_{cond} = -k(T_{x=0}) \cdot As \cdot (\partial T/\partial x)_{x=0} \tag{16}$$

$$\text{At Ra} \to 0, \quad Q_{cond} = k(T_m) \cdot As \cdot (T_h - T_c)/L \tag{17}$$

$$= h_{cond} \cdot As \cdot (T_h - T_c) \tag{18}$$

Therefore, $h_{cond} = k(T_m)/L$ where $L = (S/A)$ at $\epsilon = 1$.
We can rewrite Eq. (14) in the following form:

$$h \cdot As \cdot (T_h - T_c) = h_{cond} \cdot As \cdot (T_h - T_c) + h_{conv} \cdot As \cdot (T_h - T_c \tag{19}$$

Multiply Eq. (19) by $(S/A)/[k(T_m) \cdot As \cdot (T_h - T_c)]$ in order to nondimensionalize.
The equation becomes:

$$[h \cdot (S/A)]/k(T_m) = [h_{cond} \cdot (S/A)]/k(T_m) + [h_{conv} \cdot (S/A)]/k(T_m) \tag{20}$$

or as

$$Nu = Nu_{cond} + Nu_{conv} \tag{21}$$

Recognizing that $Nu_{cond} = Nu(Ra = 0)$ and defining $\Delta Nu = Nu_{con}$ we conclude that

$$\Delta Nu + Nu(Ra = 0) = Nu(Ra) \tag{22}$$